ACOUSTIC EMISSION MONITORING AND QUANTITATIVE EVALUATION OF DAMAGE IN CONCRETE BEAMS UNDER CREEP.

J. SALIBA*, A. LOUKILI, F. GRONDIN AND J.P. REGOIN

LUNAM Université, Ecole Centrale de Nantes, Institut de Recherche en Génie Civil et Mécanique (GeM),
UMR-CNRS 6183, 1 rue de la Noë, F-44321 Nantes, France
Email: Jacqueline.saliba@ec-nantes.fr - Web page: http://www.ec-nantes.fr

Key words: Concrete, Creep, Damage, Acoustic Emission Technique, Flexural test

Abstract: Despite the large number of studies, the mechanisms involved during creep of concrete are still not well known and particularly tensile creep which is a major issue especially in the case of special concrete structures. The objective of this study is to suggest an assessment of the damage mechanisms occurring during the different phases of creep. To achieve this, an experimental investigation is proposed on mortar and concrete beams loaded with flexural creep at high stress levels. Damage evolution under desiccation creep tests is assessed by using the acoustic emission technique. The results show a good proportionality between creep displacement and the acoustic emission activity and thus the efficiency of acoustic measurements for the estimation of the damage evolution. In addition, the results show the importance of aggregates in the fracture behaviour under desiccation creep.

1 INTRODUCTION

The study of creep in tension has shown different effect on the behaviour of concrete. On one hand, creep may relax internal tension stresses generated by shrinkage by increasing the deformation capacity to rupture and consequently reducing the risk of potential cracking in concrete [1]. On the other hand, the principal mechanism of tensile creep is due to microcracks development responsible of the decrease of the residual strength and the modification of concrete properties [2]. Many researchers tried to quantify the effect of tensile creep on the behaviour of concrete mainly by measuring the residual strength [3, 4]. A recent study conducted by the authors [5] shows, with the acoustic emission (AE) technique, a more brittle behaviour and a decrease in the fracture process zone (FPZ) in specimens subjected to flexural creep. The aim of this study is to identify and suggest an assessment of the damage mechanisms occurring during creep.

As cement-based composite, concrete can be properly represented by three phases in the microstructure: cement paste, aggregate and the interfacial transition zone (ITZ) between them. In order to well understand crack propagation in concrete, some authors had made many researches on the effect of inclusions on the fracture properties of concrete such as the aggregate content, the type of coarse aggregates, the mortar-aggregate interface… However, based on the available literature on creep, most of the experimental works have been conducted on concrete specimens. Thus, it is interesting to study the creep response of the concrete matrix in order to enhance the current knowledge of creep mechanisms of concrete and phenomena occurring at the constituents level. Fracture properties of mortar have a great influence on the fracture performance of concrete. But, how does mortar influence the creep behaviour of concrete? To examine this, an experimental

investigation is proposed on mortar and concrete beams loaded with flexural creep at high stress levels. Damage evolution under fracture and desiccation creep tests is assessed by using the AE technique. This non-destructive technique proves to be very effective, especially to check and measure micro-cracking that takes place inside a structure under mechanical loading [6]. In this study, desiccation creep tests were monitored at 70% and 85% of the maximal strength. The results aim to investigate the ranges of variation of the time response due to creep damage coupled effects and the effect of aggregate on the mechanical properties of concrete under loading.

The first part of this paper describes the experimental program performed for investigating fracture and creep tests. Then, complete load versus crack mouth opening displacement (CMOD) curves were directly obtained and fracture parameters were determined. Finally, the effect of aggregates on the fracture behaviour under creep was evaluated with the AE technique.

2 EXPERIMENTAL PROCEDURES

2.2 Materials

Concrete specimens were mixed with Portland cement CPA-CEMII 42.5, crushed limestone aggregate distributed in fine sand, with a maximum size of 5 mm and a density of 2570 kg/m^3, and crushed gravel of size 5 to 12.5 mm with a density of 2620 kg/m^3. A superplasticizer agent has been added for the workability. Table 1 shows the mix quantities of constituent materials for mortar and concrete.

Table 1: Concrete and mortar mixtures proportions

	Dosage (kg/m^3)	
Constituents	Concrete	Mortar
Gravel : 5/12,5 mm	936	-
Sand : 0/5 mm	780	1270
Cement : CEM II 42,5	350	550
Water	219.5	330
Superplasticizer	1.9	-

Concrete and mortar mixtures were characterized by a water-to-cement (W/C) ratio of 0.56. The mix proportions for mortar should represent the mortar constituents of concrete.

For the flexural tests, 800 x 200 x 100 mm^3 (*L x d x b*) concrete and mortar beams were prepared with an effective span (S) equal to 600 mm. A plate vibrator was used to compact the fresh mixture in two layers. Then, specimens were covered with a thin sheet of plastic to prevent water loss and were maintained in a climatic chamber at a temperature of 20°C and a relative humidity (RH) of 95%. 24 hours after casting, the specimens were stripped off from the moulds and kept for curing in lime water, under a temperature condition of 20°C. Before flexural tests, specimens were taken out from the curing tanks and a central notch was formed using a diamond saw cut, with a notch-to-depth ratio of 0.2 ($a_0 = d/5$).

2.1 Procedure for the three point bending test

Three point bending fracture tests were first realized to determine the maximum load so we could load the specimens in creep. The fracture test employs a load-controlled universal testing machine as per RILEM-TMC 50 recommendations [7]. The load was applied with a slow rate of 0.3 µm/s.

Flexural creep tests were then performed on frames with a capacity ranging from 5 to 50 kN. The frames were placed in a climate controlled chamber at 50 % of RH and temperature of 20 °C. The load is applied by gravity with a weight and counterweight system, which enables a fine tuning of the load [5]. The displacement was measured at midspan on notched specimens.

2.3 AE technique

The AE system comprised of an eight channel AE Win system, a general-purpose interface bus (PCI-DISP4) and a PC for data storage analysis. Eight piezoelectric transducers (resonant frequency of 150 KHz) were used to convert the mechanical waves to electrical signals. Transducers were placed

around the expected location of the fracture process zone (FPZ) to minimize errors in the AE event localization [8]. They were placed in a 3D parallelepiped position on both sides of the specimen, with silicon grease as the coupling aging (figure 1). The recorded AE amplitudes ranged from 0 to 100 dB. The detected signals were amplified with a 40 dB gain differential amplifier. In order to overcome the background noise, the signal detection threshold was set at a value of about 35 dB slightly above the background noise [8]. The acquisition system was calibrated before each test using a pencil lead break procedure HSU-NIELSEN. The effective velocity and the attenuation of acoustic waves were also calculated. For this analysis, the effective velocity was assumed to be a constant for the analysis of AE source locations even though there may be some variability depending on the wave propagation path. The effective velocity was assumed to be 3800 m/s.
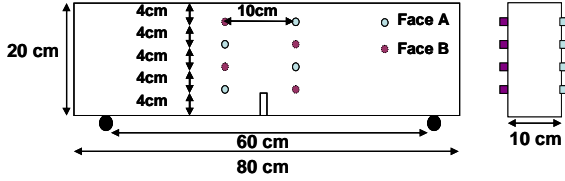

Figure 1: Specimen geometry and AE transducers position.

During the formation of a microcrack, energy is emitted as an elastic wave and propagates from the crack location to the AE transducers at the specimen surface. The locations of the AE sources are evaluated based on the arrival times of the first wave at each transducer and their respective velocity in concrete specimen.

3   FRACTURE PROPERTIES OF CONCRETE AND MORTAR

Three point bending beams of mortar and concrete were tested under loading. The mean load-CMOD curves were directly obtained (figure 2) and showed the same pattern. For the same crack width, the ultimate flexural strength (F_{max}) of concrete is higher than that of the mortar.
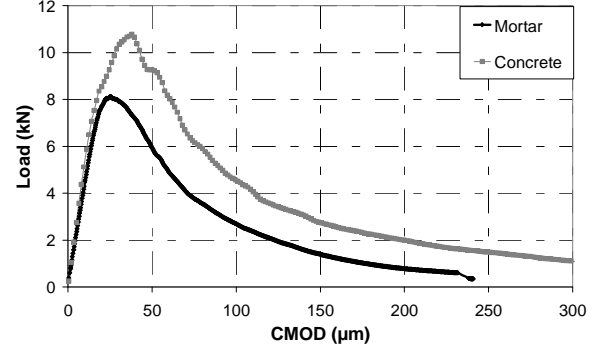

Figure 2: Mean load-CMOD curves for mortar and concrete beams.

Based on those curves, the fracture parameters as the fracture energy (G_F) were subsequently determined (table 2).

Table 2 : Fracture characteristics of concrete and mortar

	Concrete	Mortar
F_{max} (kN)	10.8	8.2
$CMOD_{peak}$ (μm)	37.9	26.5
E (Gpa)	28.1	21.9
G_F (N/m)	67.7	39.3
f_{net} (MPa)	3.9	2.9
l_{ch} (mm)	129.2	58.5

The fracture energy, calculated as the ratio of the work of fracture (W_F [N.m]) to the area of the uncracked ligament (A_{lig} [m^2]), increased with the presence of aggregate in concrete:

$$G_F = \frac{W_F}{A_{lig}} = \frac{W_0 + mg\delta_0}{b(d - a_0)} \qquad (1)$$

where W_0 [N.m] is the work dissipated in the area under the load-deflection curve, mg [N] the mass of the specimen between supports and δ_0 [m] the maximum displacement. In addition, the characteristic length (l_{ch}), defined by Hillerborg, was also calculated and showed a more brittle behaviour for mortar:

$$l_{ch} = \frac{E \times G_F}{f_t^{2}} \qquad (2)$$

where f_t [MPa] represents the tensile strength. From these phenomena, one can see that concrete presents higher fracture

3

properties than mortar because of the resistance to crack propagation enhanced due to aggregate in concrete.

4   MONITORING OF CONCRETE AND MORTAR BEAMS DURING DESICCATION CREEP TESTS

The monitoring of concrete beams under basic creep is studied in [9] and showed interesting results; however beams subjected to basic creep did not reach tertiary creep. In this paper the monitoring of desiccation creep test is only presented for concrete and mortar beams in order to have more information on the effect of the microstructure and the heterogeneities of concrete structure on creep (figure 3).

Figure 3: Desiccation creep displacement for mortar and concrete beams loaded at 70% and 85% of F_{max}.

Concrete specimens subjected to desiccation failed after 1 day at 85% (DC85) and three days at 70% (DC70). In fact, microcracking initiated due to the applied constant load begins to growth and form a crack path [10, 2, 11]. The mortar beams loaded at 70% (MDC70) did not fail even after more than four months of loading (figure 3). Creep develops fast in the first days of loading (primary creep) and then stabilizes (secondary creep). The larger the applied stress, the more important are all the kinetics and the magnitude of creep displacement. Due to desiccation, the neutral axis move upward causing an additional curvature [12, 13].

Creep displacement of mortar beams presents a more important amplitude and kinetic evolution with a more important viscous behaviour due to the presence of the aggregate in concrete that restrained creep deformation. In fact, the aggregates present an elastic behaviour and do not creep. The deformation reported to the total volume is then reduced with the diminution of the relative volume of the cement paste. The heterogeneity of concrete seems to play an important role in the fracture behaviour under creep. In order to quantify the damage evolution during creep, creep tests were monitored with the AE technique. Figure 4 presents the evolution of the AE activity during the desiccation creep tests at 70% for mortar and concrete beams. Desiccation creep tests were followed during 46 days in mortar beam and till the rupture in concrete beams. At the moment of load application, the AE activity is important with AE signals of high amplitude corresponding to microcracks in the beam and to mechanical noises at the contact between the beam and the jack. This part was removed and the AE activity was followed during the distinct phases of creep corresponding to the evolution of creep displacement into three regimes: primary creep, which corresponds to a fast decrease of strain kinetic under the initial load, followed by secondary creep, which corresponds to a quasi-constant strain kinetic, and tertiary creep in which the strain rate accelerates leading to the global failure reached with concrete beams. Those phases generate different signals covering different ranges of amplitude and corresponding to different damage mechanisms. During primary creep, the AE activity is important with AE hits of high amplitude and an important emission of AE energy (figure 4). The rate decreases in correlation with the rate of creep displacement.
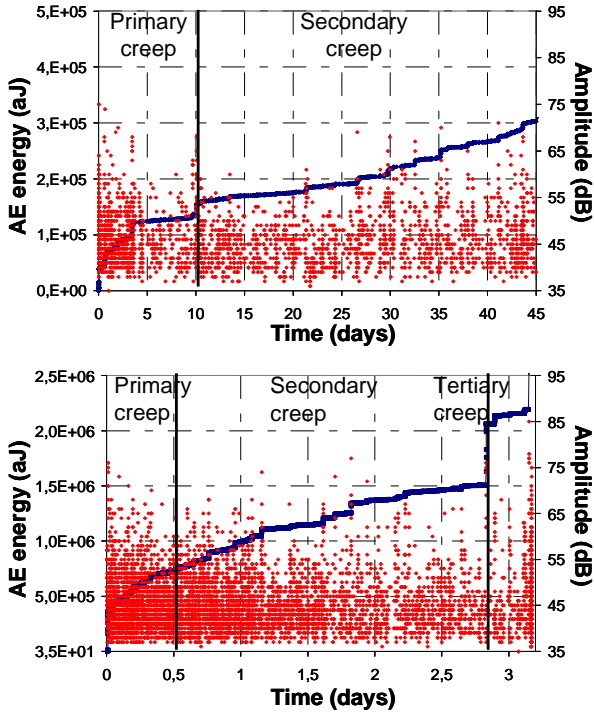
Figure 4: AE activity during desiccation creep tests for mortar and concrete beams: correlation between the cumulated AE energy and the hits amplitude.

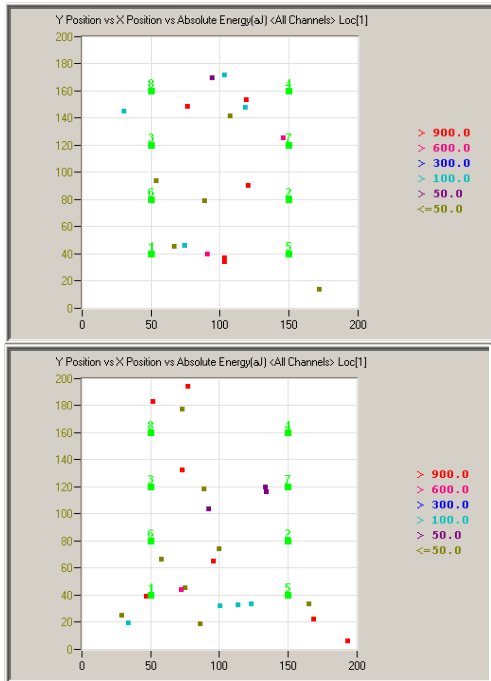During this phase, events are arbitrary distributed especially in the tension zone (figure 5).

Figure 5: Localization of AE events during primary creep for mortar (a) and concrete (b) in the plan XY.

This may correspond to the initiation and the development of microcracks inside the material as other physical mechanisms responsible of creep as water and stress redistribution in the beams and consequently microcracking.

During secondary creep, the rate of the AE activity is quasi-constant with a stable emission of AE energy (figure 4). The number of events increases with different energetic values near the notch (figure 6).
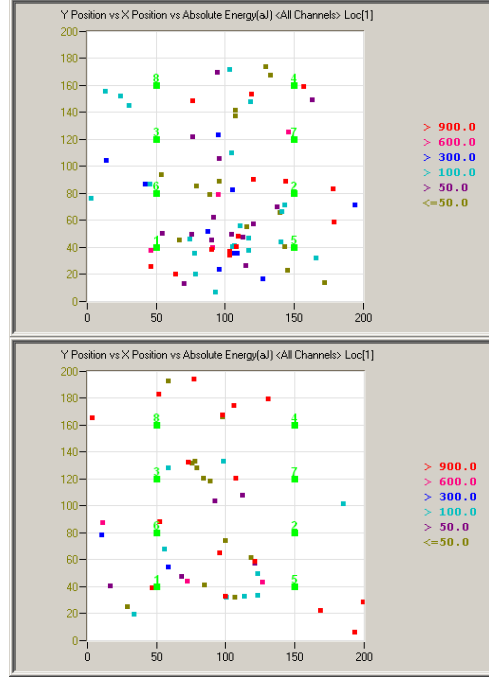

Figure 6: Localization of AE events during secondary creep for mortar (a) and concrete (b) in the plan XY.

This phase corresponds to the apparition of a new damage mechanism due to the extension and the propagation of microcracking. By analysing the energy, the amplitude and the localisation map of AE events, it is observed that the number of AE hits is less important in mortar in comparison with concrete indicating a more important damage evolution.

The localisation map of AE events along the depth of the beams (plan YZ) is also studied during secondary creep (figure 7). For mortar beam, the detected events were dispersed with events of high energy appearing especially in front of the notch and at the surfaces subjected to desiccation [14]. For concrete beams, the events presenting higher energy are localised as well at the surface as in

the width of the beams. This may be due to ITZ in concrete which is generally more brittle than the matrix [15] and constitute a zone of stress concentration. In fact, this zone contains a more important part of free water in concrete responsible of the important shrinkage when it is free to escape. The concentration of water in certain zones can cause a creep kinetics dependant of the kinetics of desiccation in concrete. Stresses are also generated by the deformation incompatibility between the aggregate and the cement paste produced by shrinkage [16, 17, 18, 19]. This could be seen on the localization maps which present events of different energy and which correspond to different damage mechanisms as microcracks in ITZ and in the matrix [20]. The stress concentrations generated in those zones are accentuated by the strain incompatibility between the aggregate and the cement paste and lead to the failure of concrete beams. In mortar beam, stresses related to the load and shrinkage are more diffuse. Aggregates play then an important role in the microcracks development at the ITZ and increase the risk of rupture under creep. The localisation of microcracks at these interfaces controls the behaviour of concrete under creep and may be responsible of it's brittleness at the rupture [5].
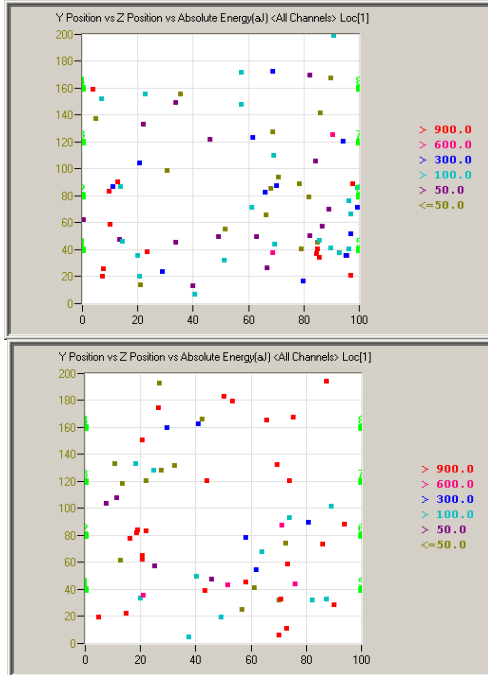

Figure 7: Localization of AE events during secondary creep for mortar (a) and concrete (b) in the plan YZ.

During tertiary creep, the AE activity increases quickly in correlation with creep displacement with the emission of very energetic signals. This phase corresponds to the coalescence and the fast propagation of microcracks where the events begin to concentrate in the cracking zone generating a localized crack and leading to the failure of the specimen in the third day. The AE signals in this phase cover different ranges of amplitude that reaches sometimes 100 dB (figure 8).
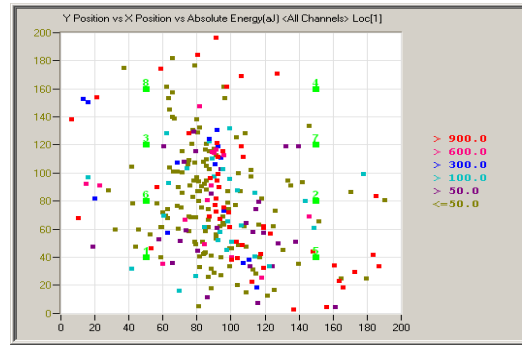

Figure 8: Localisation of AE events during tertiary creep for concrete in the plan XY.

The evolution of damage under creep seems to be different in mortar and concrete beams. Thus, in order to better understand the fracture process and the mechanisms involved, three point bending fracture tests for mortar and concrete beams are also followed with the AE technique. Fracture tests give a faster cracking process than creep tests.

5 MONITORING OF THE FRACTURE TESTS

Figure 9 presents the correlation between the load-CMOD curves and the amplitude of the AE hits for mortar and concrete during the different phases of rupture: 1) the linear elastic stage before crack initiation, 2) the nonlinear pre-peak stage of stable crack propagation preceding unstable failure, and 3) the unstable extension stage after the peak load. The AE activity is in a good correlation with the load-CMOD curve. The evolution of the acoustic emission signature during the different phases indicates different damage mechanisms. During the elastic phase, the AE activity during loading for mortar is negligible

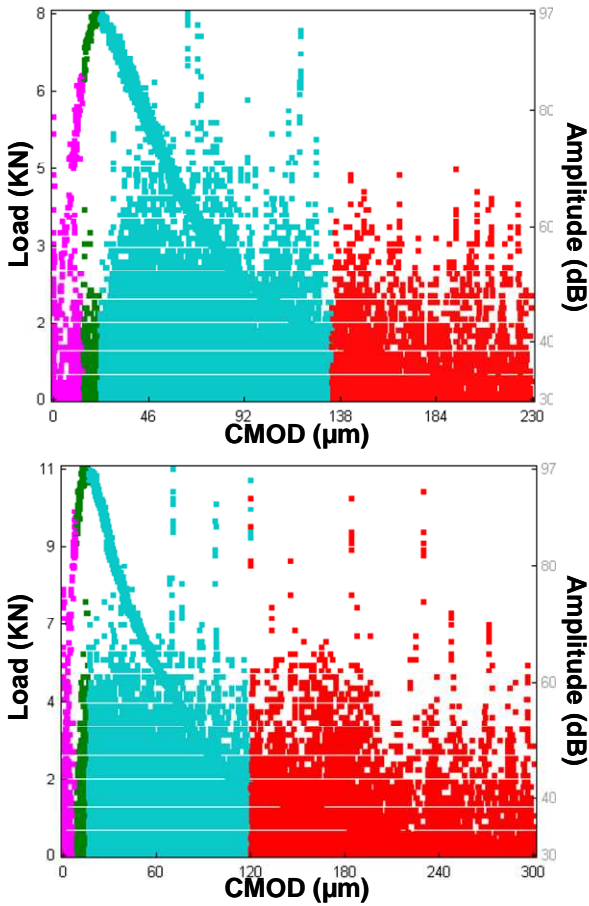however the AE activity for concrete is more important (figure 10).

Figure 9: Correlation between the load-CMOD curves and the AE hits amplitude for mortar and concrete beams.

During the nonlinear phase, some hits of weak amplitude begin to appear in mortar but always with a small rate relatively to concrete. This difference between the two materials indicates an additional mechanism in concrete. In fact, those signals of weak amplitude could be associated to microcracks at the interface between mortar and aggregate considered as the most weak and brittle zone in concrete. This is in agreement with the monitoring of creep tests where the AE activity was less important during the full test in comparison with concrete. The signals of high amplitude are globally less important. In addition, the signals of weak amplitude are also less important during creep and seem to correspond to cracks and the interface between aggregate and mortar in concrete.

During the third phase, the number of AE hits increases in both materials with the emission of high amplitude signals indicating the creation of a macrocrack (figures 9 and 10). During the terminal post-peak region, the rate of the AE activity decreases with the decrease of stress indicating the crack propagation. Note here that an unstable failure with a premature rupture was observed for mortar beams due to their brittleness.
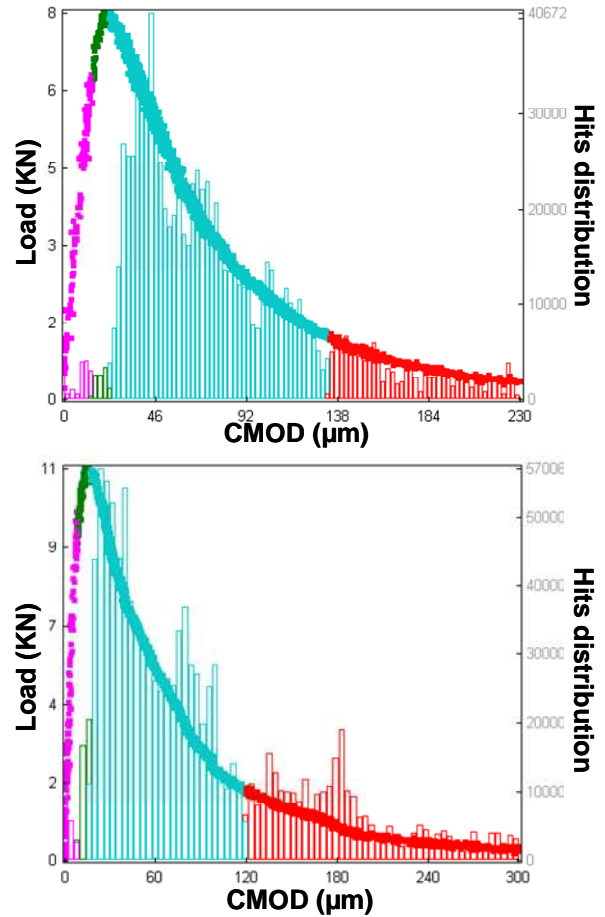

Figure 10: Correlation between the load-CMOD curves and the AE hits distribution for mortar and concrete beams.

Figure 11 presents the evolution of cumulated AE energy in correlation with the load-CMOD curves for the different materials. Energy rate jumps are observed where the presence of aggregates seems to modify or even arrests the first cracks at the ITZ. In the case of mortar beams, this barrier at the crack opening is less important and the cracks propagate more rapidly.
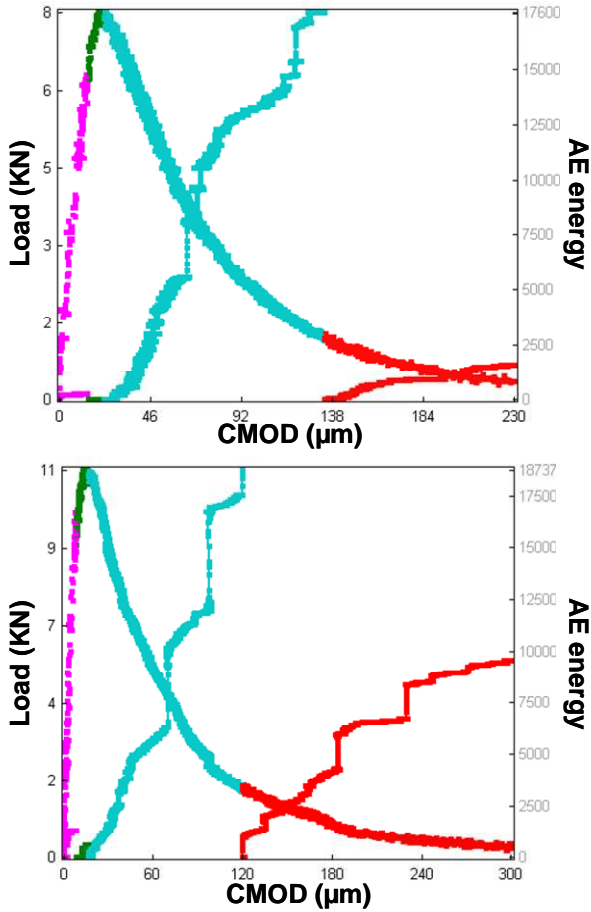
Figure 11: Correlation between the cumulated AE energy and the load-CMOD curves for mortar and concrete beams.

Figure 12: Localisation map of AE events and comparison of the width of the FPZ for mortar and concrete beams.

The AE energy is more important for concrete in correlation with the fracture energy. This is due to different mechanisms in the post peak region that adsorb additional energy [21, 22, 23]. In fact aggregates can change the orientation or the crack path in the matrix which is forced to deflect and propagate around the aggregate-mortar interface, usually more brittle. Energy release and absorption during the fracture processes of concrete are accompanied with many specific mechanisms such as micro-cracking, crack bridging, aggregate interlocking...

The localisation map of AE events for the two materials is also studied to follow the cack evolution. The detected events present different levels of energy with events of higher energy localised at the fracture core zone [24, 25] (figure 12).
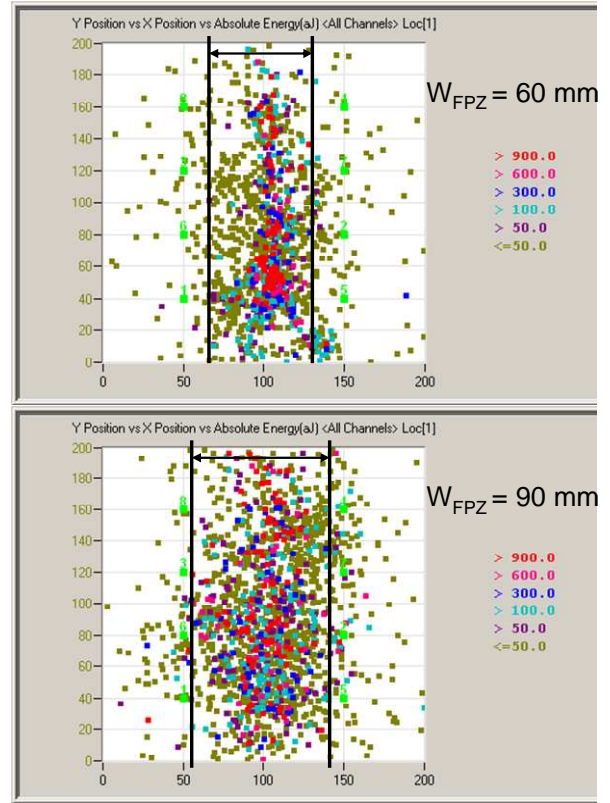
Based on the localisation map, the total number of AE events is more important in concrete. In addition, the crack path in mortar is smooth, less tortuous and more linear while the events in concrete are more dispersed, indicating a rough and complex fracture surface and a more tortuous path dominated by the distribution of aggregates and the softening mechanisms. The width of the FPZ is also measured based on the method proposed by Haidar et al. [26]. It is equal to 90 mm in concrete and decreases to 62 mm in mortar. Thus aggregates affect the fracture properties of concrete significantly by requiring higher energy for overcoming interfacial bond and increasing the width of the FPZ.

6 ESTIMATION OF THE DAMAGE EVOLUTION DURING CREEP

The stress concentration and redistribution are responsible of the failure of concrete beams and depend on the rate of loading and the loading condition. The rate of stress modifies the crack development and causes a

slow and stable increase of microcracks until the unstable condition is reached during tertiary creep. This structural damage can be correlated to the evolution of microcracks or events by relating the rate of the cumulated number of AE events (N) and the number obtained at the end of the test (N_d) in function of the time t [27]:

$$D_{EA} = \frac{N}{N_d}$$

N_d is bounded by the critical conditions ($N_d \leq N_{max}$). Figure 13 shows the evolution of the damage coefficient during flexural creep tests at 70% and 85%.
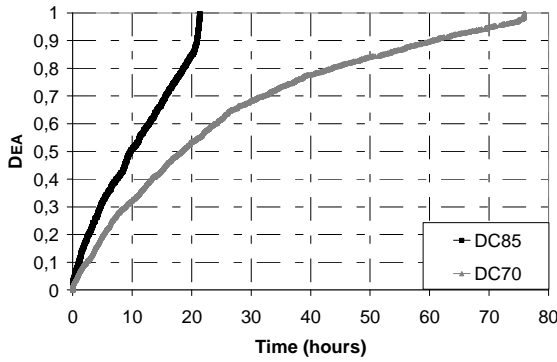

Figure 13: Evolution of the damage coefficient during desiccation creep for concrete beams.

The rate of damage measured for creep at 85% is more important in correlation with the rate of loading and the kinetics of creep displacement. Before the failure, creep displacement increases with an exponential function and residual life-time duration can be then estimated. This suggests a method to predict the rupture by following the AE activity during creep and allows estimating the degree of concrete deterioration at an early stage of the deformation before the macro-crack formation.

The quantitative understanding of the physical processes that ultimately control the fracture behaviour and the relationships between microstructure phenomena and the corresponding effects on the macroscopic behaviour is poor. It appears then necessary to take the analysis further to obtain information about the physical mechanisms, origin of the AE.

7 MULTI-VARIABLE DATA CLUSTERING ANALYSES

A multi-variable analysis of the recorded acoustic signals is proposed to discriminate the damage mechanisms in the material according to the typical AE signals and their apparition chronology. For the classification process of the monitored AE data under creep, the non-supervised method K-means associated with a principal component analysis (PCA) and the dendrogram are proposed [28]. As it is not possible to know exactly the origin of an emitted event, the K-means method allows obtaining a non-supervised classification in n class representative of the n damage mechanisms in the case of multidimensional data [29]. The PCA method is achieved in order to improve the visualisation of the classification result by reducing the dimension of the data [30]. It is then necessary to choose those descriptors wisely. The parameters were classified hierarchically with the dendrogram (figure 14). The correlation level was set to 0.9 and the descriptors used are the energy, the absolute energy, the amplitude, the rise time, the counts, the counts to peak, the average frequency and the duration of the signals.
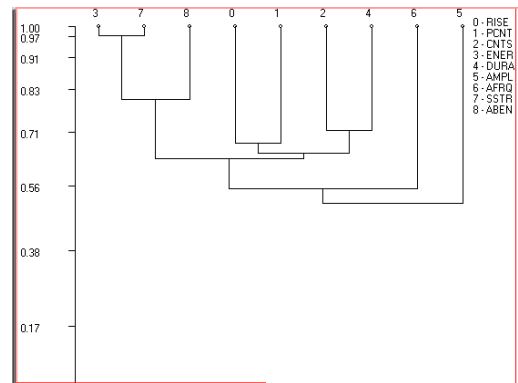

Figure 14: Correlation dendrogram of AE features.

The results of the K-means method for the concrete beam loaded at 70% are presented in figure 15: three clusters are distinguished for desiccation creep.
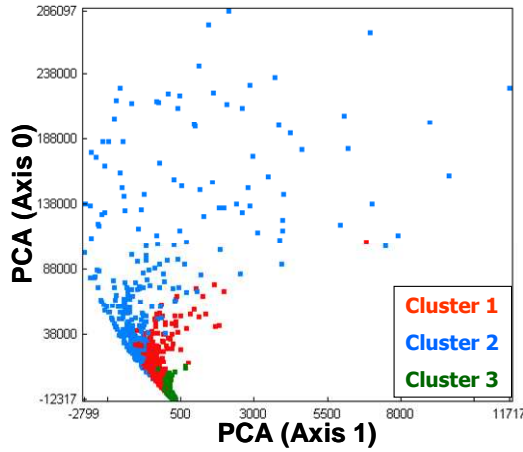
Figure 15: Visualization of the PAC clusters for desiccation creep.

Figure 17: Apparition Chronology of the clusters during desiccation creep.

In order to distinguish the origin of those clusters, the cumulated AE energy is measured for each cluster (figure 16). The first cluster corresponds to signals of weak energy while the second cluster corresponds to signals of higher energy and the third is characterized by signals of very weak energy.
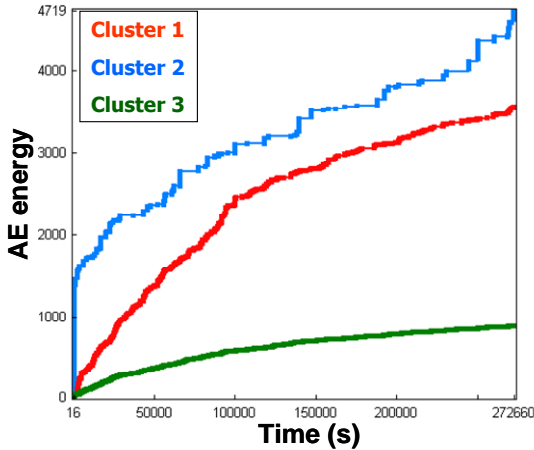

Figure 16: Cumulated energy for each cluster during desiccation creep.

The apparition chronology of those clusters shows that the third cluster appears the most important mainly at the beginning of the test and decreases with time (figure 17). And at the contrary, the second cluster which presents the most important AE energy has few AE hits. The first cluster is the most distinguished damage mechanism and involves much more numerous AE hits.
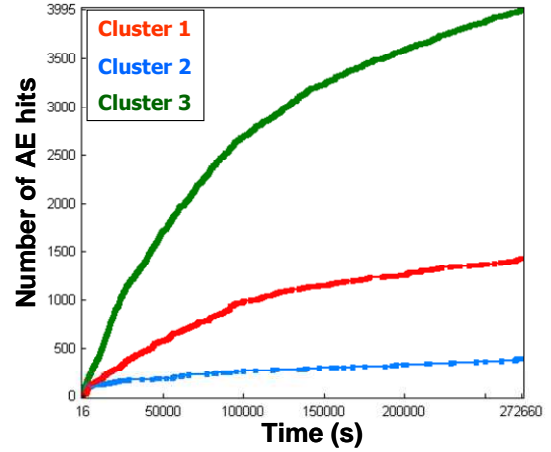
Figure 18 shows the experimental distribution of the AE hits amplitude for each cluster. The AE hits amplitude distribution situated at 50% of the max value for the first cluster is between 42 and 55 dB and can be associated to microcracking at the matrix-aggregate interface [31]. For the second cluster, it is between 45 and 68 dB and can be associated to micro-cracking in the matrix [31]. For the third cluster, it is between 38 and 47 dB. Based on the analyses of the AE parameters, this cluster corresponds to signals due to the desiccation and liquid transfer in concrete (sorption and desorption) [32].
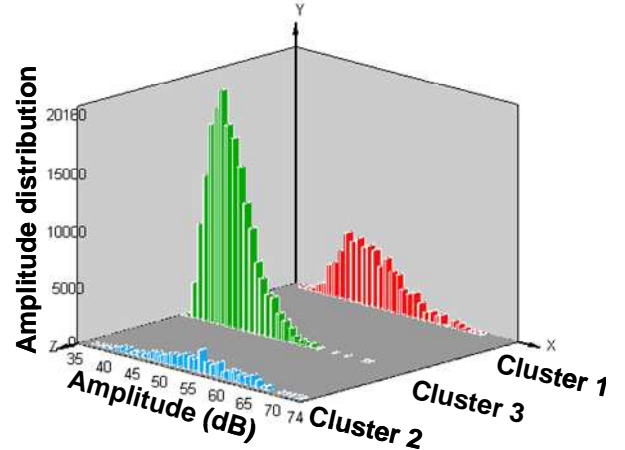

Figure 18: Experimental AE hits amplitude distributions for each cluster

Through this approach, we have shown that it is possible, using the AE technique, to identify the most critical damage mechanisms leading to the final failure of concrete.

10

8 CONCLUSIONS

The fracture properties of mortar and concrete were tested by similar three-point bending beams. For mortar, the post peak section of the load-CMOD curve is much steeper and the critical crack mouth opening displacement is smaller. The maximal strength and the fracture energy increases in concrete due to the deflection of the propagating cracks in matrix and the bigger fracture process zone. AE technique provides useful information about crack propagation inside concrete beams during fracture and creep tests. The AE activity is proportional to creep displacement and permits to distinguish the three distinct phases of creep. The aggregates play an important role in the crack propagation during desiccation creep due to the gradient deformation between the aggregate and the matrix and the stress redistribution.

9 REFERENCES

[1] Bissonnette B., Pigeon M., 2000. Le comportement viscoélastique du béton en traction et la compatibilité déformationnelle des réparations. *Materials and Structures.* 33 :108-118.

[2] Rossi P., Godart N., Robert J.L, Gervais J.P., Bruhat D., 1994. Investigation of the basic creep of concrete by acoustic emission. *Materials and Structures.* 27:510-514.

[3] Omar M., Loukili A., Pijaudier-cabot G., Le Pape Y., 2009. Creep-damage coupled effects: experimental investigation on bending beams with various sizes. *Journal of materials in civil engineering.* 21(2):65-72.

[4] Liniers A.D., 1987. Microcracking of concrete under compression and its influence on tensile strength. *Materials and structures.* 20:111-116.

[5] Saliba J., Loukili A., Grondin F., Regoin J.-P., 2012. Experimental study of creep-damage coupling in concrete by acoustic emission technique. *Materials and Structures.* 45(9):1389-1401.

[6] Denarié E., Cécot C., Huet C., 2006. Characterization of creep and crack growth interactions in the fracture behaviour of concrete. *Cement and Concrete Research.* 36:571- 575.

[7] RILEM 50-FMC Recommendation, 1985. Determination of fracture energy of mortar and concrete by means of three-point bend test on notched beams. *Materials and Structures.* 18:285-290.

[8] RILEM TC212-ACD Recommendation, 2010 Acoustic Emission and related NDE Techniques for Crack Detection and Damage Evaluation in concrete. *Materials and structures.* 43:1177-1181.

[9] Saliba J., Loukili A., Grondin F., Regoin J.-P., 2012. Identification of damage mechanisms in concrete under creep by the acoustic emission technique. *Cement and Concrete Research.* Submitted

[10] Ngab A.S., Slate F.O., Nilson A.H., 1981. Microcracking and time-dependent strains in high strength concrete. *ACI Materials Journal.* 11:262-268.

[11] Bazant Z.P., Gettu R., 1992. Rate effects and load relaxation in static fracture of concrete. *ACI Materials Journal.* 89(5):456-468.

[12] Bazant Z.P., Chern J.C., 1985. Concrete creep at variable humidity: constitutive law and mechanism. *Matériaux et Constructions.* 18(103):1-20.

[13] Bazant Z.P., Yunping X., 1994. Drying creep of concrete: constitutive model and new experiments separating its mechanisms. *Materials and Structures.* 27:3-14.

[14] Bazant Z.P., Raftshol W.J., 1982. Effect of cracking in drying and shrinkage specimens. *Cement and Concrete Research.* 12:209-226.

[15] Zimbelmann R., 1985. A contribution to the problem of cement-aggregate bond. *Cement & concrete Research.* 15(5):801-808.

[16] Bisschop J., van Mier J.G.M., 2002. How to study drying shrinkage microcracking in cement-based materials using optical and scanning electron microscopy? *Cement and Concrete Research.* 32:279-287.

[17] Wong H.S., Zobel M., Buenfeld N.R., Zimmerman R.W., 2009. The influence of

the interfacial transition zone and microcracking on the diffusivity, permeability and sorptivity of cement-based materials after drying. *Magazine of Concrete Research*. 61:571-589

[18] Idiart A.E., Lopez C.M., Carol I., 2011. Chemo-mechanical analysis of concrete cracking and degradation due to external sulfate attack: A meso-scale model. *Cement & Concrete Composites*. 33:411-423.

[19] Grassl P., Jirasek M., 2010. Meso-scale approach to modelling the fracture process zone of concrete subjected to uniaxial tension. *International Journal of Solids and Structures*. 47:957-968.

[20] Saliba J., 2012. Contribution of the Acoustic Emission technique in the understanding and the modelling of the coupling between creep and damage in concrete. *PHD thesis at Ecole Centrale de Nantes* (in French).

[21] Landis E.N., 1999. Micro-macro fracture relationships and acoustic emissions in concrete. *Construction and Building Materials*. 13:65-72.

[22] Wu K., Chen B., Yao W., 2001. Study of the influence of aggregate size distribution on mechanical properties of concrete by acoustic emission technique. *Cement & Concrete Research*. 31:919-923.

[23] Chen B., Liu J., 2004. Effect of aggregate on the fracture behavior of high strength concrete. *Construction and Building Materials*. 18:585-590.

[24] Otsuka K., Date H., 2000. Fracture process zone in concrete tension specimen. *Engineering Fracture Mechanics*. 65:111-131.

[25] Wu K., Chen B., Yao W., 2000. Study on the AE characteristics of fracture process of mortar, concrete and steel-fiber-reinforced concrete beams. *Cement and Concrete Research*. 30:1495-1500.

[26] Haidar K., Pijaudier-Cabot G., Dubé J.F., Loukili A., 2005. Correlation between the internal length, the fracture process zone and size effect in model materials. *Materials and Structures*. 38:201-210.

[27] Carpinteri A, Valente S, Zhou FP, Ferrara G, Melchiorri G, 1997. Tensile and flexural creep rupture tests on partially-damaged concrete specimens. *Materials and Structures*. 30:269-276.

[28] Kostopoulos V., Loutas T.H., Kontsos A., Sotiriadis G., Pappas Y.Z., 2003. On the identification of the failure mechanisms in oxide/oxide composites using acoustic emission. *NDT&E International*. 36:571-580.

[29] Likas A., Vlassis N., Verbeek J.J., 2003. The global K-means clustering algorithm. *Pattern Recognition*. 36:451-461.

[30] Oja E., 1989. Neural networks, principal components, and subspaces. *International Journal of Neural Systems*. 1:61-68.

[31] Rossi P., Robert J.L., Gervais J.P., Bruhat D., 1989. Identification of the physical mechanisms underlying acoustic emissions during the cracking of concrete. *Materials and Structures*. 22:194-198.

[32] Chotard T., Quet A., Ersen A., Smith A., 2006. Application of the acoustic emission technique to characterise liquid transfer in a porous ceramic during drying. *Journal of the European Ceramic Society*. 26:1075-1084.